Mon. Not. R. astr. Soc. (1985) **216,** 173–192

Bright extragalactic radio sources at 2.7 GHz – III. The all-sky catalogue

J. V. Wall *Royal Greenwich Observatory, Herstmonceux Castle, Hailsham, East Sussex BN27 1RP*

J. A. Peacock *Royal Observatory, Blackford Hill, Edinburgh EH9 3HJ*

Accepted 1985 April 9. Received 1985 April 9; in original form 1984 November 27

Summary. We catalogue the brightest extragalactic radio sources at 2.7 GHz. The complete sample comprises 233 sources found in the major centimetre-wavelength surveys carried out at ANRAO/Parkes, NRAO/Greenbank, and MPIfR/Bonn; the sample covers 9.81 sr and has limits $S_{2.7}$=2.0 Jy and $|b|>10°$. A critical re-analysis of the data shows that 227 (97 per cent) have optical identifications and 171 (73 per cent) have measured redshifts. The implications of the catalogue statistics for the luminosity functions of different radio-source populations are considered.

1 Introduction

This paper continues the series in which samples of extragalactic radio sources are used to study the cosmological history of radio sources (Peacock & Wall 1981, 1982; PWI & PWII). The primary aim is to provide databases relevant to finding the radio luminosity function and its dependence on epoch, but 'complete' samples are vital in almost all branches of extragalactic astronomy because the selection effects can be simply quantified for statistical investigations. In this series, we have concentrated on sources selected at centimetre wavelengths to counter a historical bias towards objects from the earlier surveys at low frequencies, in particular 3CR Apart from technical problems (the effects of confusion and resolution in 3CR are well documented by Laing, Riley & Longair 1983), surveys such as 3CR are strongly biased against the class of object known variously as 'flat-spectrum' or 'cm-excess'. These sources, with emission dominated by compact, self-absorbed components, appear in large numbers in surveys made above ~1.4 GHz. Samples selected at the higher frequencies are therefore essential to obtain a complete picture of the radio-source population.

PWI described a sample of 168 sources with $S_{2.7}\geq 1.5$ Jy over the northern hemisphere. The present catalogue is complete to 2 Jy over essentially the whole sky with $|b|\geq 10°$. What this provides is an increase by a factor 3 over PWI on the number of sources at this level, yielding important constraints on the population of *nearby* luminous objects which are intrinsically rare. It therefore achieves a better determination of the high-luminosity end of the local luminosity

function, allowing more precise comparison with the high-redshift population revealed by fainter samples. It is frustrating to note that an all-sky catalogue is the best we can now do in this respect: sampling effects restrict our knowledge of the local Universe, unless we can wait a Hubble time for new data.

This is not the first all-sky catalogue, but previous efforts [Robertson (1973) at 408 MHz and Kühr *et al.* (1981) at 5 GHz] were of limited usefulness due to the incomplete nature of the optical data. Ideally, we require all objects to have a measured redshift or a reliable redshift estimate, perhaps from galaxy photometry; this information exists for approximately 82 per cent of our sample. For the remainder, estimates can be made to sufficient accuracy, given the limited sample size; our conclusions depend only weakly on these estimates being correct. We provide what we believe is the closest possible approach to a complete and reliable data set; we hope that our conclusions from its analysis will serve as a stimulus towards the sort of observational effort devoted with great success to extending the optical data for 3CR (e.g. Spinrad, Stauffer & Butcher 1981).

2 The catalogue

The catalogue appears in Table 1, and the sources are plotted on a Flamsteed equal-area projection of the sky in Fig. 1. The columns of Table 1 are:

(i) IAU name.
(ii) Other name.
(iii) & (iv) Right ascension (1950.0) and uncertainty in seconds of time.
(v) & (vi) Declination (1950.0) and uncertainty in arcseconds. A *C* in column 4 indicates that the position quoted is the mid-point of a double source without a central component. In this case, the position error quoted against declination (Column 6) applies to both right ascension and declination, and is 0.1 times the total angular extent of the source. Laing *et al.* (1983) show that this approximates the rms deviation of the optical identification from the mid-point. If the position is not given as a centroid in column (4) the position is for an unresolved component. In some cases, however, the resolution used may be low (~arcminutes for many southern sources) and the derived position is effectively a centroid. Thus, the formal errors on the centroid position are only appropriate for sources much smaller than the beam.
(vii) Reference for position. 1. Perley 1982; 2. Ulvestad *et al.* 1981; 3. Morabito *et al.* 1982; 4. Morabito *et al.* 1983; 5. Large *et al.* 1981; 6. Fomalont & Moffet 1971; 7. Hunstead 1972; 8. Jenkins, Pooley & Riley 1977; 9. Laing 1981; 10. Burch 1979; 11. Longair 1975; 12. Pooley & Henbest 1974; 13. Northover 1973; 14. Riley & Pooley 1975; 15. PWII; 16. Hargrave 1974; 17. Northover 1976; 18. Turland 1975; 19. Birkinshaw, Laing & Peacock 1981; 20. Elsmore & Ryle 1976; 21. Hargrave & McEllin 1975; 22. Riley & Branson 1973; 23. Correction of PWII misprint (unpublished VLA data); 24. Adgie, Crowther & Gent 1972; 25. Schilizzi & McAdam 1975; 26. Cameron 1971; 27. Christiansen *et al.* 1977; 28. Ekers *et al.* 1978; 29. Willis, Strom & Wilson 1974; 30. Waggett, Warner & Baldwin 1977; 31. Prestage, Peacock & Wall, in preparation.
(viii), (ix), (x) Flux densities at 1.4, 2.7 and 5 GHz.
(xi) Spectral index $\alpha_{2.7}^{5}$, defined in the sense $S_\nu \propto \nu^{-\alpha}$.
(xii) Optical classification:

Q QSO confirmed by spectrum or variability (and including BL Lac objects),
Q? Stellar object on position,
G Galaxy confirmed by extended image,
G? Very faint object; presumed galaxy (see Section 2.2),
EF Empty field.

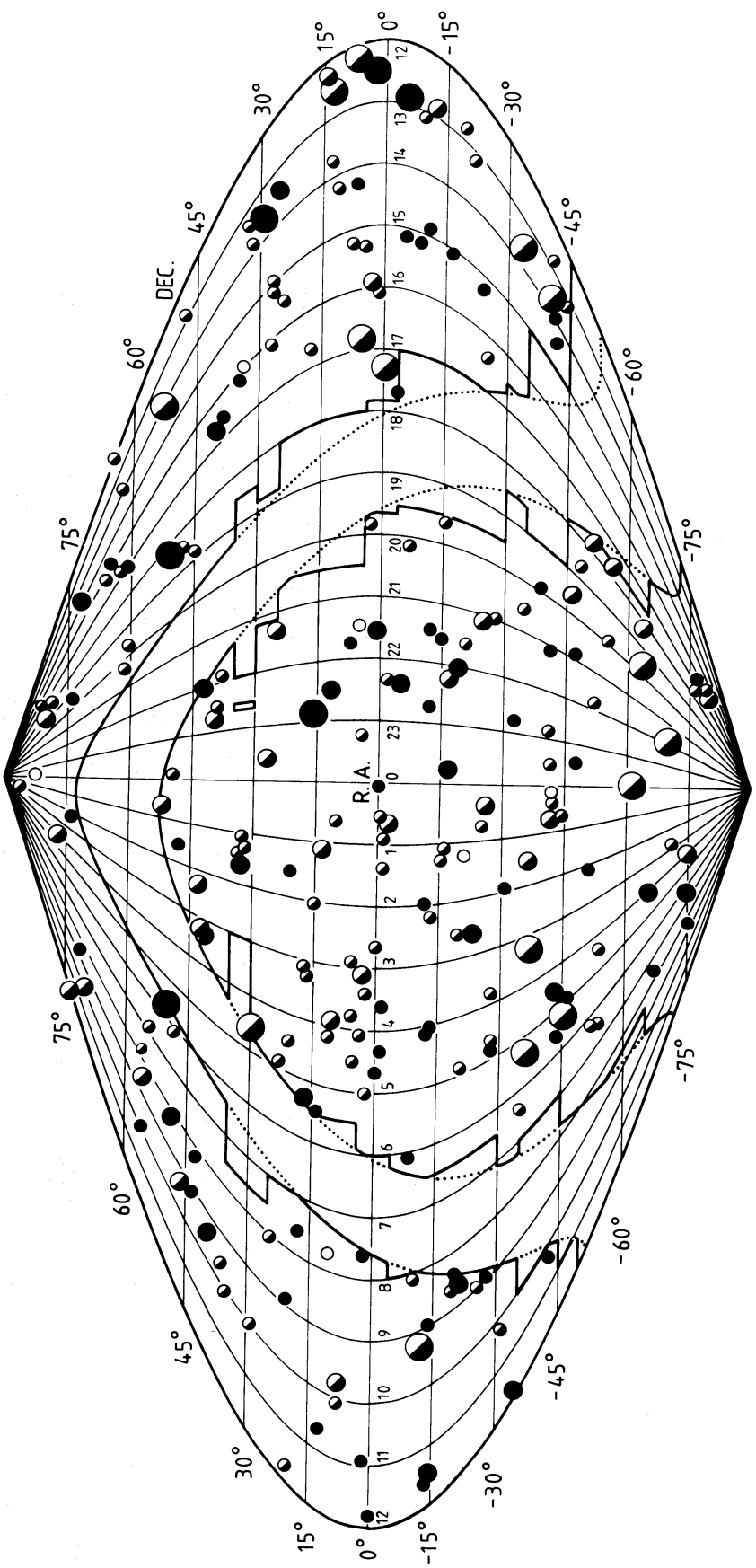

Figure 1. The area covered by the catalogue, which is complete to $S_{2.7}=2.0$ Jy over 9.81 sr. The sources in the catalogues are represented by symbols corresponding in size to three 2.7-GHz flux-density ranges: ⩾10 Jy; 4–10 Jy; 2–4 Jy. QSOs are represented by filled circles, galaxies by half-filled circles, and empty fields by open circles.

Table 1. The catalogue.

(1)	(2)	(3) R.A.	(4)	(5) Dec.	(6)	(7)	(8) S(1.4)	(9) S(2.7)	(10) S(5.0)	(11) ∝	(12) ID	(13) V	(14) z
0003-00	3C2	00 03 48.84	0.03	-00 21 06.0	0.4	24	3.54	2.40	1.41	0.86	Q	19.4	1.037
0008-42		00 08 21.30	0.01	-42 09 50.6	0.1	1	5.40	2.47	1.31	1.03	EF		1.600*
0022-42		00 22 15.42	0.01	-42 18 40.7	0.1	1	3.02	2.84	1.77	0.77	G?	20.6	0.661*
0023-26	OB-238	00 23 18.91	0.01	-26 18 49.3	0.1	1	9.00	5.80	3.76	0.70	G	19.5	0.398*
0034-01	3C15	00 34 30.56	0.02	-01 25 37.8	0.4	4	4.30	2.56	1.57	0.79	G	15.3	0.073
0035-02	3C17	00 35 47.18	0.02	-02 24 09.5	0.3	4	6.25	4.04	2.59	0.72	G	18.0	0.220
0038+09	3C18	00 38 14.57	0.12	09 46 56.1	4.1	6	4.26	3.00	1.62	1.00	G	18.5	0.188
0039-44		00 39 46.86	0.27	-44 30 28.6	2.4	7	4.30	2.08	1.17	0.93	G	18.5	0.251*
0040+51	3C20	00 40 19.99	C	51 47 08.1	5.0	8	10.79	6.51	4.18	0.72	G	19.0	0.350
0043-42		00 43 54.50	0.20	-42 24 01.0	3.0	5	9.10	5.00	2.93	0.87	G	16.0	0.053
0045-25	NGC253	00 45 05.60	0.20	-25 33 37.0	3.0	5	6.30	3.52	2.40	0.62	G	7.0	.0010
0055-01	3C29	00 55 01.57	0.02	-01 39 39.4	0.3	4	5.22	3.46	2.16	0.76	G	14.1	0.045
0104+32	3C31	01 04 39.17	0.02	32 08 44.3	0.6	8	5.22	3.53	2.10	0.84	G	12.2	0.017
0105-16	3C32	01 05 48.78	0.07	-16 20 21.1	1.2	7	3.80	2.25	1.14	1.10	G	20.1	0.525*
0106+13	3C33	01 06 14.94	C	13 04 26.4	24.0	9	12.59	8.02	5.03	0.76	G	15.2	0.060
0114-21	OC-224	01 14 25.95	0.01	-21 07 55.0	0.1	1	4.10	2.23	1.24	0.95	EF		1.600*
0116+31	4C31.04	01 16 47.25	0.01	31 55 05.8	0.1	1	2.54	2.12	1.46	0.61	G	14.5	0.059
0117-15	3C38	01 17 59.84	0.14	-15 35 57.3	2.1	7	4.70	2.72	1.56	0.90	G?	21.0	0.794*
0123-01	3C40	01 23 27.41	0.02	-01 36 16.7	0.3	31	6.42	3.29	1.88	0.91	G	12.3	0.018
0123+32	3C41	01 23 54.70	C	32 57 38.7	2.3	11	3.49	2.26	1.46	0.71	G	22.0	0.794
0131-36		01 31 43.54	0.02	-36 44 57.2	1.3	28	7.10	5.60	4.08	0.51	G	13.0	0.030
0133+20	3C47	01 33 40.42	0.01	20 42 10.6	0.5	12	3.68	2.00	1.16	0.88	Q	18.1	0.425
0133+47	OC457	01 33 55.11	0.01	47 36 12.8	0.1	1	2.17	2.22	3.26	-0.62	Q	18.0	0.860
0134+32	3C48	01 34 49.83	0.01	32 54 20.5	0.1	1	15.29	9.08	5.37	0.85	Q	16.2	0.367
0157-31	OC-397	01 57 58.51	0.11	-31 07 50.6	1.5	7	3.70	2.37	1.44	0.81	Q?	19.6	2.032*
0159-11	3C57	01 59 30.27	0.07	-11 47 00.2	1.3	7	2.90	2.00	1.35	0.64	Q	16.4	0.669
0202+14	4C15.05	02 02 07.40	0.01	14 59 51.0	0.1	1	3.40	3.00	2.30	0.43	G?	22.1	1.202*
0208-51		02 08 56.97	0.02	-51 15 07.5	0.2	4		3.56	3.21	0.17	Q	17.5	1.003
0210+86	3C61.1	02 10 45.20	C	86 05 08.2	18.0	9	6.06	3.77	1.68	1.31	G	19.0	0.186
0212+73		02 12 49.94	0.01	73 35 40.1	0.1	1		2.39	2.20	0.13	Q?	19.5	1.928*
0213-13	3C62	02 13 11.61	0.14	-13 13 24.0	3.6	7	5.00	2.79	1.77	0.74	G	18.0	0.200*
0220+42	3C66B	02 20 01.73	0.02	42 45 54.6	0.3	13	10.25	5.23	3.75	0.54	G	12.8	0.022
0235-19	OD-159	02 35 24.90	0.07	-19 45 29.3	1.2	7	4.40	2.41	1.41	0.87	G?	20.3	0.575*
0237-23	OD-263	02 37 52.79	0.01	-23 22 06.3	0.1	1	7.02	4.90	3.30	0.64	Q	16.6	2.223
0240-00	NGC1068	02 40 07.09	0.04	-00 13 30.7	0.6	24	4.87	3.13	1.93	0.78	G	9.0	.0041
0252-71		02 52 26.50	0.60	-71 16 43.0	4.0	5	5.90	3.10	1.54	1.14	G	18.0	0.200*
0255+05	3C75	02 55 05.10	0.50	05 50 44.0	8.0	6	6.22	3.30	1.94	0.86	G	13.6	0.024
0305+03	3C78	03 05 49.05	0.01	03 55 13.1	0.1	1	7.24	5.34	3.60	0.64	G	12.8	0.029
0307+16	3C79	03 07 11.35	0.02	16 54 36.8	1.0	14	4.59	2.50	1.41	0.93	G	18.5	0.256
0314+41	3C83.1B	03 14 56.79	0.02	41 40 32.6	0.3	14	9.35	4.92	3.53	0.54	G	13.3	0.026
0316+16	CTA21	03 16 09.14	0.01	16 17 40.4	0.1	1	7.60	4.77	2.93	0.79	G?	22.0	1.259*
0316+41	3C84	03 16 29.56	0.01	41 19 51.9	0.1	1	12.76	9.64	47.20	-2.58	G	11.9	0.017
0320-37	For A	03 20 46.80	0.30	-37 23 06.0	4.0	27		98.00	71.00	0.52	G	5.1	.0057
0325+02	3C88	03 25 18.90	0.40	02 23 22.0	0.4	6	4.85	3.18	1.95	0.79	G	14.0	0.030
0336-01	CTA26	03 36 58.95	0.01	-01 56 16.9	0.1	1	2.30	2.02	2.30	-0.21	Q	18.4	0.852
0347+05	4C05.16	03 47 06.97	0.11	05 42 35.2	2.6	7	3.25	2.00	1.24	0.78	G?	20.9	0.759*
0349-27	OE-283	03 49 36.90	2.40	-27 52 50.0	30.0	25	5.20	2.89	2.01	0.59	G	15.8	0.066
0356+10	3C98	03 56 10.49	C	10 17 16.4	25.0	8	9.56	5.80	3.29	0.92	G	14.4	0.031
0403-13	OF-105	04 03 14.20	0.20	-13 16 21.0	3.0	5	3.30	3.15	3.24	-0.05	Q	17.2	0.571
0404+76	4C76.03	04 04 00.13	0.16	76 48 52.5	0.2	15		4.05	2.79	0.60	G	22.2	1.380*
0404+03	3C105	04 04 48.07	0.04	03 32 49.7	0.6	24	4.93	3.54	2.39	0.64	G	18.5	0.089
0405-12	OF-109	04 05 27.45	0.05	-12 19 32.4	0.7	3	2.80	2.35	1.81	0.42	Q	17.1	0.574
0407-65		04 07 58.09	0.14	-65 52 49.2	1.3	7	15.00	6.50	3.28	1.11	Q?	18.0	0.871*
0409-75		04 09 58.94	0.31	-75 14 57.1	2.0	7	13.50	7.23	4.25	0.86	G?	21.5	1.000*
0410+11	3C109	04 10 54.85	0.01	11 04 39.5	0.5	14	4.09	2.50	1.77	0.56	G	17.9	0.306
0420-01		04 20 43.54	0.01	-01 27 28.8	0.1	1	1.70	2.15	2.14	0.01	Q	17.8	0.915
0428-53		04 28 00.00	2.00	-53 56 00.0	20.0	27	5.83	3.84	3.40	0.20	G	13.2	0.039
0428+20	OF247	04 28 06.86	0.01	20 31 09.1	0.1	1	3.81	3.18	2.30	0.53	G	20.0	0.219
0430+05	3C120	04 30 31.60	0.01	05 14 59.5	0.1	1	5.48	3.00	8.60	-1.71	G	14.1	0.033
0433+29	3C123	04 33 55.30	C	29 34 18.8	2.0	12	45.67	27.57	16.20	0.86	G	19.9	0.218
0438-43		04 38 43.18	0.01	-43 38 53.1	0.1	1	6.80	6.20	7.00	-0.20	Q	18.8	2.852
0440-00	OF-67	04 40 05.29	0.01	-00 23 20.6	0.1	1	3.18	3.73	3.13	0.28	Q	18.5	0.844
0442-28	OF-271	04 42 37.40	0.50	-28 15 18.0	7.0	6	7.10	3.84	2.16	0.93	G	17.4	0.151*
0451-28	OF-285	04 51 15.13	0.01	-28 12 29.3	0.1	1	2.50	2.38	2.50	-0.08	Q	18.5	2.564
0453-20	OF-289	04 53 14.13	0.15	-20 38 56.4	2.0	7	4.70	2.79	1.78	0.73	G	13.0	0.035

Table 1 – *continued*

(1)	(2)	(3) R.A.	(4)	(5) Dec.	(6)	(7)	(8) S(1.4)	(9) S(2.7)	(10) S(5.0)	(11) α	(12) ID	(13) V	(14) z
0453+22	3C132	04 53 42.05	C	22 44 43.4	1.0	8	3.25	2.10	1.13	1.01	G	19.0	0.214
0454-46		04 54 24.19	0.03	-46 20 38.5	0.2	4	2.60	2.36	2.04	0.24	Q	18.0	0.858
0500+01	OG3	05 00 45.18	0.01	01 58 53.8	0.1	1	2.21	2.47	1.85	0.47	G?	21.4	0.995*
0518+16	3C138	05 18 16.53	0.01	16 35 26.9	0.1	1	8.88	7.10	4.04	0.92	Q	17.9	0.759
0518-45	Pic A	05 18 23.00	0.50	-45 49 44.0	6.0	27	66.00	29.00	15.00	1.07	G	16.0	0.035
0521-36		05 21 12.90	0.06	-36 30 16.5	1.1	7	18.60	12.50	9.23	0.49	G	16.8	0.062
0528+13	OG147	05 28 06.76	0.01	13 29 42.2	0.1	1	2.19	2.97	3.86	-0.43	Q?	19.5	1.928*
0537-44		05 37 21.00	0.01	-44 06 46.8	0.1	1	2.70	3.84	3.80	0.02	Q	15.5	0.894
0538+49	3C147	05 38 43.51	0.01	49 49 42.8	0.1	1	22.05	13.14	8.18	0.77	Q	16.9	0.545
0605-08	OH-10	06 05 36.03	0.01	-08 34 20.3	0.1	1	2.50	2.70	3.39	-0.37	Q?	18.0	0.871*
0605+48	3C153	06 05 44.46	0.04	48 04 49.0	0.4	24	4.01	2.33	1.35	0.89	G	18.5	0.277
0620-52		06 20 34.30	0.40	-52 39 42.0	4.0	5	3.40	2.10	1.23	0.87	G	14.5	0.051
0625-53		06 25 19.23	0.12	-53 39 25.5	1.6	7	6.70	3.70	1.80	1.17	G	13.0	0.054
0625-35	OH-342	06 25 20.80	0.20	-35 27 20.0	3.0	5	4.50	2.90	2.09	0.53	G	14.0	0.055
0637-75		06 37 23.42	0.07	-75 13 37.4	0.2	4	6.70	4.51	5.49	-0.32	Q	15.8	0.651
0651+54	3C171	06 51 11.05	0.05	54 12 50.4	0.4	24	3.66	2.02	1.16	0.90	G	18.8	0.238
0735+17	OI158	07 35 14.13	0.01	17 49 09.3	0.1	1	1.92	2.00	2.05	-0.04	Q	14.9	0.424
0736+01	OI61	07 36 42.51	0.01	01 44 00.2	0.1	1	2.89	2.30	2.06	0.18	Q	16.5	0.191
0742+10	OI471	07 42 48.47	0.01	10 18 32.5	0.1	1	3.17	3.74	3.57	0.08	EF		2.000*
0743-67		07 43 22.19	0.05	-67 19 09.1	0.3	4	5.30	2.74	1.51	0.97	Q	16.4	0.395
0744+55	DA240	07 44 34.82	0.07	55 56 28.3	0.6	29		2.84		0.78	G	14.2	0.036
0802+24	3C192	08 02 32.31	C	24 18 54.9	10.0	8	4.89	3.30	2.13	0.71	G	15.5	0.060
0806-10	3C195	08 06 29.90	0.06	-10 19 09.7	1.4	7	3.40	2.49	1.60	0.72	G	17.8	0.182*
0809+48	3C196	08 09 59.42	0.04	48 22 07.2	0.4	24	13.85	7.75	4.35	0.94	Q	17.6	0.871
0814+42	OJ425	08 14 51.67	0.01	42 32 07.7	0.1	1	2.48	2.24	1.68	0.47	Q	16.9	0.486*
0825-20	OJ-242	08 25 03.49	0.06	-20 16 25.9	1.0	7	3.70	2.10	1.18	0.94	Q	18.0	0.871*
0831+55	4C55.16	08 31 04.38	0.01	55 44 41.4	0.1	1	8.04	7.54	5.60	0.48	G	17.5	0.242
0834-20	OJ-257.5	08 34 24.60	0.01	-20 06 30.4	0.1	1	3.50	4.15	3.42	0.31	Q	19.0	2.752
0834-19	OJ-158.1	08 34 56.15	0.03	-19 41 25.4	0.4	2	4.60	2.50	1.51	0.82	G?	20.7	0.692*
0836+71	4C71.07	08 36 21.56	0.01	71 04 22.5	0.1	1		3.15	2.57	0.33	Q?	16.5	0.394*
0842-75		08 42 10.73	0.26	-75 29 36.3	1.6	7	4.30	2.15	1.38	0.72	Q	18.9	0.524
0851+20	OJ287	08 51 57.25	0.01	20 17 58.4	0.1	1	1.59	3.42	2.61	0.44	Q	14.0	0.306
0858-27	OJ-297	08 58 31.70	0.30	-27 56 33.0	4.0	5	2.20	2.00	1.38	0.60	Q?	16.2	0.336*
0859-25	OJ-299	08 59 36.63	0.13	-25 43 38.8	1.7	7	5.80	3.30	1.70	1.08	G	21.0	0.794*
0859-14	OJ-199	08 59 54.94	0.01	-14 03 38.9	0.1	1	3.10	2.93	2.29	0.40	Q	16.6	1.327
0906+43	3C216	09 06 17.25	0.04	43 05 59.4	0.4	24	3.76	2.42	1.78	0.50	Q	18.5	0.668
0915-11	Hyd A	09 15 41.50	0.30	-11 53 06.0	7.0	6	37.40	23.50	13.50	0.90	G	14.8	0.052
0917+45	3C219	09 17 50.70	0.02	45 51 44.2	0.1	10	8.02	4.40	2.29	1.06	G	17.3	0.174
0923+39	4C39.25	09 23 55.32	0.01	39 15 23.5	0.1	1	2.52	4.60	8.90	-1.07	Q	17.9	0.699
0936+36	3C223	09 36 50.86	0.03	36 07 34.7	0.7	14	3.35	2.09	1.29	0.78	G	17.1	0.137
0945+07	3C227	09 45 07.80	0.50	07 39 09.0	5.0	6	7.40	4.30	2.60	0.82	G	16.3	0.086
0951+69	M82	09 51 41.95	0.01	69 54 57.5	0.1	16	7.94	5.66	3.94	0.59	G	8.4	.0014
0954+55	4C55.17	09 54 14.36	0.01	55 37 16.4	0.1	1	3.52	2.63	2.27	0.24	Q	17.7	0.909
0958+29	3C234	09 58 57.38	0.01	29 01 37.4	0.2	14	5.35	2.96	1.54	1.06	G	17.1	0.185
1003+35	3C236	10 03 05.39	0.01	35 08 48.0	0.2	8	3.24	2.03	1.32	0.70	G	16.0	0.099
1005+07	3C237	10 05 22.02	0.03	07 44 58.6	0.4	24	6.25	3.50	1.93	0.97	G?	21.3	0.912*
1015-31	OL-327	10 15 53.39	0.01	-31 29 11.3	0.1	1	3.50	2.22	1.32	0.84	G?	20.2	0.550*
1017-42		10 17 56.23	0.12	-42 36 21.9	1.3	7	4.10	2.33	1.20	1.08	Q	19.0	1.280
1040+12	3C245	10 40 06.00	0.03	12 19 15.1	0.4	24	3.06	2.00	1.41	0.57	Q	17.3	1.029
1055+01	4C01.28	10 55 55.32	0.01	01 50 03.5	0.1	1	3.10	3.02	3.07	-0.03	Q	17.7	0.888
1127-14	OM-146	11 27 35.67	0.01	-14 32 54.4	0.1	1	6.20	6.50	7.25	-0.18	Q	16.9	1.187
1136-13	OM-161	11 36 38.51	0.08	-13 34 05.4	1.1	3	4.10	2.80	1.88	0.65	Q	17.8	0.554
1142+19	3C264	11 42 29.58	0.02	19 53 02.7	0.4	17	5.78	3.27	2.36	0.53	G	12.8	0.021
1148-00	4C-00.47	11 48 10.13	0.01	-00 07 13.3	0.1	1	2.90	2.58	1.95	0.45	Q	17.6	1.982
1151-34	OM-386	11 51 49.44	0.01	-34 48 47.2	0.1	1	6.40	4.18	2.74	0.69	Q	17.5	0.258
1157+73	3C268.1	11 57 49.30	C	73 17 26.5	4.0	8	7.04	4.05	2.63	0.70	G	22.0	0.970*
1203+64	3C268.3	12 03 54.08	0.03	64 30 18.5	0.1	12	3.53	2.00	1.16	0.88	G	19.0	0.371
1216+06	3C270	12 16 51.20	1.00	06 06 13.0	6.0	6	17.50	12.80	9.04	0.56	G	10.4	.0069
1222+13	M84	12 22 31.58	0.02	13 09 50.7	1.5	8	6.24	4.30	2.72	0.74	G	8.7	.0028
1226+02	3C273	12 26 33.25	0.01	02 19 43.3	0.1	1	38.84	38.90	40.00	-0.05	Q	12.8	0.158
1228+12	Vir A	12 28 17.56	0.01	12 40 02.0	0.3	18	214.00	120.00	67.60	0.93	G	8.7	.0038
1245-19	ON-176.2	12 45 45.22	0.01	-19 42 57.5	0.1	1	5.50	3.94	2.47	0.76	G?	19.5	0.398*
1246-41	NGC4696	12 46 03.27	0.15	-41 02 21.4	1.7	7	4.10	2.21	1.33	0.82	G	11.2	.0090
1251-12	3C278	12 51 59.60	0.50	-12 17 08.0	6.0	6	6.80	4.50	2.54	0.93	G	13.5	0.015
1253-05	3C279	12 53 35.84	0.01	-05 31 08.0	0.1	1	10.40	11.20	16.10	-0.59	Q	17.8	0.538

Table 1 – *continued*

(1) IAU	(2) Name	(3) R.A.	(4)	(5) Dec.	(6)	(7)	(8) S(1.4)	(9) S(2.7)	(10) S(5.0)	(11) α	(12) ID	(13) V	(14) z
1254+47	3C280	12 54 41.36	C	47 30 32.1	1.3	12	5.08	2.86	1.53	1.02	G	22.0	0.996
1306-09	OP-10	13 06 02.20	0.20	-09 34 33.0	3.0	5	4.40	2.80	1.88	0.65	G?	20.5	0.631*
1308-22	3C283	13 08 57.40	0.03	-22 00 46.7	0.4	2	5.40	2.43	1.09	1.30	G?	21.5	1.000*
1318-43	NGC5090	13 18 14.00	C	-43 26 57.0	30.0	25	5.86	3.09	1.71	0.96	G	14.5	0.011
1322-42	Cen A	13 22 32.23	C	-42 45 25.0	40.0	26		128.00	61.00	1.20	G	7.0	.0008
1323+32	4C32.44	13 23 57.92	0.01	32 09 43.0	0.1	1	4.56	3.35	2.31	0.60	G?	19.0	0.316*
1328+25	3C287	13 28 15.93	0.01	25 24 37.4	0.1	1	6.72	4.60	3.08	0.65	Q	17.7	1.055
1328+30	3C286	13 28 49.66	0.01	30 45 58.6	0.1	1	14.78	10.38	7.48	0.53	Q	17.3	0.849
1333-33	IC4296	13 33 47.18	0.07	-33 42 39.8	0.9	3	11.96	10.06	6.19	0.79	G	11.1	0.013
1345+12	4C12.50	13 45 06.17	0.01	12 32 20.3	0.1	1	5.01	3.80	2.89	0.44	G	17.0	0.122
1350+31	3C293	13 50 03.23	0.03	31 41 32.6	0.4	24	4.42	2.93	1.87	0.73	G	14.4	0.045
1355-41		13 55 56.83	0.12	-41 38 16.7	1.5	7	4.60	2.49	1.40	0.93	Q	16.0	0.313
1358+62	4C62.22	13 58 58.36	0.01	62 25 06.7	0.1	1	4.32	2.69	1.77	0.68	G	20.2	0.525*
1409+52	3C295	14 09 33.50	0.04	52 26 13.0	0.4	24	22.18	11.94	6.48	0.99	G	20.1	0.461
1414+11	3C296	14 14 26.36	0.04	11 02 18.6	1.2	19	4.32	2.73	1.71	0.76	G	12.2	0.024
1416+06	3C298	14 16 38.77	0.03	06 42 20.9	0.4	2	5.66	2.70	1.52	0.93	Q	16.8	1.439
1424-41		14 24 46.73	0.07	-41 52 54.4	1.0	3	3.50	2.63	2.12	0.35	Q?	17.5	0.668*
1453-10	OQ-190	14 53 12.32	0.07	-10 56 51.0	1.5	7	3.70	2.50	1.41	0.93	Q	17.4	0.940
1458+71	3C309.1	14 58 56.64	0.01	71 52 11.2	0.1	20	8.50	5.36	3.33	0.77	Q	16.8	0.904
1502+26	3C310	15 02 46.88	0.02	26 12 35.4	0.7	8	7.67	3.10	1.26	1.46	G	15.3	0.054
1504-16	OR-107	15 04 16.42	0.01	-16 40 59.3	0.1	1	2.70	2.30	1.96	0.26	Q	18.5	0.876
1508-05	4C-05.64	15 08 14.98	0.01	-05 31 49.0	0.1	1	3.90	2.50	2.33	0.11	Q	17.0	1.191
1510-08	OR-107	15 10 08.90	0.01	-08 54 47.6	0.1	1	3.00	3.00	3.25	-0.13	Q	16.3	0.361
1511+26	3C315	15 11 30.81	0.02	26 18 39.4	0.4	8	3.87	2.10	1.31	0.77	G	16.8	0.108
1514+07	3C317	15 14 17.08	0.07	07 12 16.2	1.9	7	5.35	2.20	0.93	1.40	G	13.5	0.035
1514-24	Ap Lib	15 14 45.28	0.01	-24 11 22.6	0.1	1	2.70	2.10	1.94	0.13	Q	15.0	0.049
1518+04	4C04.51	15 18 44.73	0.03	04 41 05.5	0.4	24	4.01	2.20	1.00	1.28	G?	22.8	1.820*
1529+24	3C321	15 29 33.50	0.03	24 14 26.5	1.0	8	3.59	2.20	1.09	1.14	G	16.0	0.096
1547-79		15 47 39.15	0.41	-79 31 42.4	2.1	7	4.00	2.28	1.35	0.85	G	18.0	0.200*
1549-79		15 49 28.38	0.21	-79 05 17.8	0.3	4	6.20	4.02	4.50	-0.18	G	18.8	0.288*
1559+02	3C327	15 59 58.60	2.00	02 06 24.0	30.0	25	8.95	5.04	2.81	0.95	G	15.9	0.104
1600+33	4C33.38	16 00 11.91	0.01	33 35 09.6	0.1	1	2.36	2.26	1.51	0.65	EF		2.000*
1602+01	3C327.1	16 02 12.96	0.02	01 25 58.7	0.3	4	4.07	2.14	1.11	1.07	G	20.5	0.480*
1607+26	CTD93	16 07 09.29	0.01	26 49 18.6	0.1	1	4.43	3.04	1.56	1.08	G?	21.0	0.794*
1609+66	3C330	16 09 13.90	C	66 04 22.8	6.0	8	6.98	3.76	2.35	0.76	G	20.3	0.549
1610-77		16 10 51.75	0.10	-77 09 52.6	0.3	4	5.00	3.37	5.55	-0.81	Q	19.0	1.710
1611+34	OS319	16 11 47.92	0.01	34 20 19.8	0.1	1	2.92	2.45	2.67	-0.14	Q	17.5	1.401
1622-25	OS-237.8	16 22 44.11	0.01	-25 20 51.5	0.1	1	1.60	2.27	2.20	0.19	G?	21.9	1.202*
1633+38	4C38.41	16 33 30.63	0.01	38 14 10.1	0.1	1	2.01	2.53	4.08	-0.78	Q	18.0	1.814
1634+62	3C343	16 34 01.08	0.01	62 51 41.6	0.1	1	5.17	2.71	1.50	0.96	Q	20.6	0.988
1637-77		16 37 05.50	0.90	-77 09 55.0	4.0	5	6.50	3.77	2.58	0.62	G	16.0	0.043
1637+62	3C343.1	16 37 55.31	0.01	62 40 34.3	0.1	1	4.66	2.26	1.20	1.03	G	20.7	0.750
1637+82	NGC6251	16 37 56.95	0.01	82 38 18.5	0.1	30		2.17		0.70	G	13.0	0.024
1641+39	3C345	16 41 17.61	0.01	39 54 10.8	0.1	1	6.30	6.08	10.90	-0.95	Q	16.0	0.594
1641+17	3C346	16 41 34.55	0.04	17 21 20.6	0.5	24	3.64	2.20	1.34	0.80	G	17.2	0.161
1648+05	Her A	16 48 40.10	0.50	05 04 28.0	5.0	6	44.43	24.60	12.41	1.11	G	16.9	0.154
1704+60	3C351	17 04 03.51	0.07	60 48 31.3	0.6	9	3.52	2.05	1.21	0.86	Q	15.3	0.371
1717-00	3C353	17 17 56.80	0.20	-00 55 49.0	4.0	5	56.22	33.80	20.20	0.84	G	15.4	0.030
1733-56		17 33 20.40	1.20	-56 32 26.0	10.0	27	8.40	5.20	3.32	0.73	G?	17.0	0.126*
1740-51		17 40 27.00	0.30	-51 43 25.0	2.0	5		4.60	2.95	0.72	G	19.2	0.347*
1741-03	OT-68	17 41 20.62	0.01	-03 48 48.9	0.1	1	1.00	3.05	3.63	-0.28	Q?	18.5	1.135*
1803+78		18 03 39.18	0.01	78 27 54.3	0.1	1		2.36	2.63	-0.18	G?	13.8	0.029*
1814-63		18 14 46.13	0.20	-63 47 00.9	1.6	7	14.20	7.50	4.29	0.91	G	16.0	0.063
1828+48	3C380	18 28 13.54	0.04	48 42 40.5	0.4	24	14.11	10.00	6.19	0.78	Q	16.8	0.691
1832+47	3C381	18 32 24.40	C	47 24 36.5	7.0	14	3.79	2.33	1.29	0.96	G	17.5	0.161
1839-48		18 39 27.10	0.30	-48 39 39.0	3.0	5	3.70	2.00	1.26	0.75	G	16.5	0.100*
1842+45	3C388	18 42 35.45	0.02	45 30 21.6	0.2	12	5.57	3.15	1.77	0.94	G	15.7	0.091
1845+79	3C390.3	18 45 37.57	0.04	79 43 06.4	0.1	21	12.33	6.64	4.32	0.70	G	14.4	0.057
1928+73	4C73.18	19 28 49.35	0.01	73 51 44.9	0.1	1		3.42	3.34	0.04	Q	15.5	0.360
1932-46		19 32 18.91	0.12	-46 27 23.9	1.2	7	13.40	6.54	3.47	1.03	G	18.9	0.302*
1934-63		19 34 47.65	0.14	-63 49 34.7	1.6	7	16.00	11.10	6.45	0.88	G	18.4	0.183
1938-15	OV-164	19 38 24.80	0.20	-15 31 34.0	4.0	5	6.90	3.80	2.29	0.82	G?	21.5	1.000*
1939+60	3C401	19 39 38.84	0.05	60 34 32.6	0.5	8	4.75	2.79	1.52	0.99	G	19.1	0.201
1949+02	3C403	19 49 44.13	0.09	02 22 41.5	2.1	7	5.85	3.68	2.35	0.73	G	15.4	0.059
1954-55		19 54 18.90	0.40	-55 17 42.0	4.0	5	7.00	3.74	2.31	0.78	G	16.3	0.060

Table 1 – *continued*

(1)	(2)	(3) R.A.	(4)	(5) Dec.	(6)	(7)	(8) S(1.4)	(9) S(2.7)	(10) S(5.0)	(11) α	(12) ID	(13) V	(14) z
1954-38		19 54 39.06	0.01	-38 53 13.3	0.1	1	1.59	2.00	2.00	0.00	Q	17.5	0.630
2008-06	OW-15	20 08 33.70	0.01	-06 53 01.8	0.1	1	3.65	2.20	1.33	0.82	G?	21.6	1.047*
2021+61	OW637	20 21 13.30	0.01	61 27 18.1	0.1	1	2.20	2.17	2.31	-0.10	G	19.5	0.227
2032-35	OW-354	20 32 37.20	0.12	-35 04 29.6	1.4	7	6.40	3.70	1.88	1.10	G?	21.5	1.000*
2052-47		20 52 50.13	0.03	-47 26 19.6	0.2	4	3.00	2.20	2.45	-0.17	Q	17.8	1.491
2058-28	OW-297.8	20 58 39.50	2.50	-28 13 15.0	30.0	25	6.70	3.10	1.96	0.74	G	14.6	0.038
2104-25	OX-208	21 04 25.30	2.50	-25 37 58.0	30.0	25	12.00	7.30	4.23	0.89	G	15.8	0.037
2106-41		21 06 19.39	0.01	-41 22 33.4	0.1	1	1.98	2.11	2.28	-0.13	Q?	20.0	2.512*
2121+24	3C433	21 21 31.00	C	24 51 36.0	10.0	12	11.68	7.00	3.62	1.07	G	15.5	0.102
2128+04	OX46	21 28 02.61	0.01	04 49 04.3	0.1	1	3.98	3.12	2.07	0.67	EF		2.000*
2128-12	OX-148	21 28 52.67	0.01	-12 20 20.6	0.1	1	1.80	2.00	2.00	0.00	Q	16.0	0.501
2134+00	OX57	21 34 05.21	0.01	00 28 25.1	0.1	1	3.13	7.60	12.38	-0.79	Q	18.0	1.936
2135-14	OX-158	21 35 00.10	0.30	-14 46 27.0	4.0	5	3.00	2.00	1.36	0.63	Q	15.5	0.200
2135-20	OX-258	21 35 01.32	0.01	-20 56 03.7	0.1	1	3.78	2.49	1.50	0.82	G	19.4	0.380*
2145+06	4C06.69	21 45 36.08	0.01	06 43 40.9	0.1	1	2.97	3.10	4.57	-0.63	Q	16.5	0.990
2150-52		21 50 48.17	0.18	-52 04 23.9	1.8	7	4.20	2.10	1.17	0.95	G?	22.2	1.380*
2152-69		21 52 58.60	0.80	-69 55 50.0	8.0	5	30.39	19.27	12.44	0.71	G	14.0	0.027
2153+37	3C438	21 53 45.42	C	37 46 13.1	2.0	8	6.70	3.26	1.54	1.22	G	19.2	0.290
2200+42	BL Lac	22 00 39.36	0.01	42 02 08.6	0.1	1	4.60	5.21	4.75	0.15	Q	14.5	0.069
2203-18	OY-106	22 03 25.73	0.01	-18 50 17.1	0.1	1	6.20	5.20	4.24	0.33	Q	19.0	0.618
2211-17	3C444	22 11 42.51	0.07	-17 16 33.7	1.2	7	7.90	4.52	2.08	1.26	G	18.0	0.153
2221-02	3C445	22 21 15.50	2.00	-02 21 16.0	30.0	25	5.59	3.46	2.25	0.70	G	15.8	0.056
2223-05	3C446	22 23 11.05	0.04	-05 12 17.4	0.7	3	6.00	4.40	4.31	0.03	Q	18.4	1.404
2229+39	3C449	22 29 07.60	0.03	39 06 03.4	0.6	19	3.62	2.50	1.39	0.95	G	13.2	0.017
2230+11	CTA102	22 30 07.80	0.01	11 28 22.8	0.1	1	6.01	5.30	3.50	0.67	Q	17.5	1.037
2243+39	3C452	22 43 32.81	0.01	39 25 27.6	0.2	14	10.53	5.94	3.26	0.97	G	16.0	0.081
2243-12	OY-172.6	22 43 39.80	0.01	-12 22 40.3	0.1	1	2.54	2.74	2.38	0.23	Q	17.3	0.630
2245-32	OY-376	22 45 51.53	0.01	-32 51 42.2	0.1	1	1.37	2.01	1.80	0.18	Q	18.6	2.268
2250-41		22 50 12.25	0.15	-41 13 44.4	1.7	7	5.20	2.34	1.27	0.99	G	19.0	0.316*
2251+15	3C454.3	22 51 29.52	0.01	15 52 54.3	0.1	1	11.84	10.00	23.30	-1.37	Q	16.1	0.860
2314+03	3C459	23 14 02.27	0.03	03 48 55.2	0.4	24	4.17	2.36	1.30	0.97	G	17.6	0.220
2326-47		23 26 33.72	0.02	-47 46 51.8	0.2	4	2.82	2.34	2.46	-0.08	Q	16.0	1.299
2331-41		23 31 45.37	0.13	-41 42 02.5	1.3	7	5.70	2.66	1.52	0.91	G	18.0	0.200*
2335+26	3C465	23 35 58.95	0.01	26 45 16.4	0.1	22	7.51	4.00	2.12	1.03	G	13.2	0.029
2342+82		23 42 06.35	0.02	82 10 01.3	0.1	23		2.33	1.30	0.95	EF		1.000*
2345-16	OZ-176	23 45 27.69	0.01	-16 47 52.6	0.1	1	1.20	4.08	3.47	0.26	Q	18.0	0.600
2352+49	OZ488	23 52 37.79	0.01	49 33 26.8	0.1	1	2.93	2.21	1.77	0.36	G	19.0	0.237
2356-61		23 56 30.00	C	-61 11 30.0	36.0	27	23.70	10.22	4.43	1.36	G	16.0	0.096

(xiii) *V* magnitude.

(xiv) Redshift; * indicates an estimate (Section 2.2).

2.1 SOURCE SELECTION

The basic selection of Table 1 was from the Parkes 2.7-GHz survey, which covers some 7 sr of sky at declinations south of +25°, omitting regions within ~10° of the galactic plane. Bolton, Wright & Savage (1979) list the 14 parts of this survey, all of which have completeness limits much fainter than the 2.0-Jy selection criterion of the present catalogue. To extend the coverage over the remainder of the sky, the 2.7-GHz sample compiled in PWI was used, with two modifications:

(i) The 2.7-GHz flux-density scale was changed from that used by Kellermann, Pauliny-Toth & Tyler (1968; KPT) to the Parkes flux-density scale. In PWI, we determined $\langle S_{KPT}/S_{PARKES}\rangle = 0.988 \pm 0.006$, and the flux densities of sources common to KPT and Table 1 therefore differ by ~1 per cent.

(ii) For sources in PWI with both a Parkes and KPT flux density, the Parkes measurement was adopted.

As in PWI, all sources within 10° of the galactic plane were rejected. In addition, regions occupied by the Large and Small Magellanic Clouds (a total of 0.04 sr) were excluded. Finally, two sources identified with galactic objects (H II regions and supernova remnants) were removed. The total area covered (Fig. 1) is 9.81 sr.

This selection procedure produced a list of 231 sources which is complete (discounting variability) for sources of small angular size. For sources extended enough to be resolved by the beam of the survey instrument, however, there is a possible incompleteness. The relevant HPBWs at 2.7 GHz are 8 arcmin for the Parkes 64-m telescope, 11 arcmin for the NRAO 43-m telescope and 5 arcmin for the Bonn 100-m telescope. For sources much larger than these limits, the beam-broadening correction to the total flux density applied by fitting a Gaussian may not be adequate. These problems should be minimized in the region covered by Parkes ($\delta \leqslant 25°$), since this area was originally surveyed at 408 MHz – allowing detection of any very extended sources up to ~1° across (e.g. Cen A≡NGC 5128; For A≡NGC 1316; PKS 1333−33≡IC 4296). These observations formed the basis for the first generation of 2.7-GHz measurements, and we therefore consider it unlikely that our sample has omitted any very extended sources from the Parkes zone. For $\delta \geqslant 35°$, the 2.7-GHz measurements for the 5-GHz 'S' surveys on which our sample is based were made with the MPIfR 100-m telescope, which could in itself lead to incompleteness for sources larger than ~10 arcmin. In fact, the 5-GHz finding survey $35° \leqslant \delta \leqslant 70°$ was made with the NRAO 92-m telescope (HPBW 2.7 arcmin at 5 GHz) while at $\delta \geqslant 70°$, the MPIfR 100-m telescope (HPBW 2.2 arcmin) was used. Sources of even a few arcminutes extent would be heavily resolved. The 5-GHz completeness limit is generally 0.3–0.4 Jy, but as high as 0.65 Jy in some areas of the sky. Thus, potential members of our 2.7-GHz sample may well be omitted from the 'S' surveys if they have beam-broadening factors ≥2, corresponding to angular sizes ≥5 arcmin. This incompleteness can be countered to some extent by using the 1.4-GHz survey of Bridle *et al.* (1972), the most complete available for northern sources of large angular size. We considered all sources with equivalent Gaussian diameters ≥5 arcmin NS or EW and 1.4-GHz flux densities ≥2.76 Jy (our limit assuming $\alpha=0.5$); 12 extragalactic sources satisfying these criteria lay in our survey region, of which eight were already in the sample. Two of the remaining four sources were known to be blends of unrelated objects, which left 0130+30 (M33) and 0744+55 (DA 240). To these candidates should be added two 'giant' sources from the unpublished Cambridge 151-MHz survey which were outside the Bridle *et al.* survey zone: 0945+73 (Mayer 1979) and 1637+82 (NGC 6251; Waggett *et al.* 1977). Flux densities at 2.7 GHz for these sources were determined as follows. For DA 240, using the data of Bridle *et al.* (1972) and Willis *et al.* (1974) we obtained $S_{2.7}=2.84$ Jy ($\alpha=0.78$). For 0945+73 the spectrum is uncertain due to resolution corrections on a 10.6-GHz flux density; the interpolated 2.7-GHz flux density lies between 1.5 and 1.9 Jy, below the present sample limit but above the PWI limit. For NGC 6251, the extended lobes have an extrapolated flux density of $S_{2.7}=1.45$ Jy ($\alpha=0.70$), plus 0.72-Jy nuclear emission. Thus, DA 240 and NGC 6251 should be added to our sample; both these sources, together with 0945+73, should have appeared in the PWI sample. With regard to nearby galaxies, the total flux density of M33 is very uncertain, but we are justified in omitting it since it is part of our local group (as are M31 and the Magellanic Clouds which we also exclude). Any remaining incompleteness can be estimated by comparing the numbers of sources with $\theta \geqslant 5$ arcmin in the zone covered by Parkes and in the north. In $\delta \leqslant 25°$, 19 are observed, yielding a predicted number for $\delta \geqslant 25°$ of 8, whereas five are observed. Therefore, if we have not found all the northern giants, it is unlikely that more than three remain to be added to the sample.

The flux densities in columns (8) and (10) of Table 1 were selected from catalogues in the following order of preference:

1.4 GHz: Bridle *et al.* (1972); Pauliny-Toth, Wade & Heeschen (1966); Parkes; OSU surveys.
5 GHz: Parkes; NRAO/MPIfR 'S' surveys.

No corrections for different flux-density scales were made, as these are generally small (~1 per cent) at frequencies of 1.4 GHz and above. The spectral index in column (11) is $\alpha_{2.7}^{5}$, with the exception of the giant sources discussed above.

2.2 OPTICAL DATA

The majority of the sources in Table 1 have well-established identifications given in a variety of compilations. The most useful of these were by Laing *et al.* (1983; updated version from R. A. Laing) and Smith & Spinrad (1980), which contained identifications for 84 of our sources; all these were judged to be certain. We next took candidate identifications from the compilations of Burbidge & Crowne (1979) and Hewitt & Burbidge (1980). Agreement between radio and optical positions was checked and the identification accepted if the agreement was better than 3 times the combined rms measurement errors, provided these were $\lesssim$1 arcsec. For the remaining 102 sources without a firm identification, references from the compilation of Véron-Cetty & Véron (1983) were consulted, and positional agreement for candidate identifications again considered. For 34 of these sources, new optical positions were measured by Prestage & Peacock (1983). Finally, we were able to use recent VLA (Prestage, Peacock & Wall, in preparation) and CCD (Wall *et al.*, in preparation) data to provide firm identifications for some sources for which the correct optical candidate had been either uncertain due to poor radio data or invisible at the limit of sky survey plates.

As a result of this critical assessment, we consider the identification status of only seven sources to remain in doubt: 0407–65, 0409–75, 1733–56, 1740–51, 1839–48, 1954–55, and 2150–52. These all lack high-resolution radio observations, so that the expected optical position is poorly known. (This situation applies to many southern objects, but in most cases either the suggested identification is sufficiently bright as to leave no doubt, or there is an unimportant ambiguity between several faint cluster galaxies.) For the above sources we have accepted candidate identifications even when there are substantial differences between radio and optical positions, on the grounds that many of the sources are certain to be extended.

We divided the identifications into two categories: G or Q, depending on whether the optical object is clearly extended or stellar (and confirmed as the correct identification by spectroscopy or variability). No distinction is made in the catalogue between QSOs and BL Lac objects (see Section 3.1). Stellar identifications without spectroscopy are designated Q?, and the remaining (usually very faint) objects are designated G?, on the well-established grounds that the Q/Q? magnitude distribution for bright radio sources peaks well before the optical limit, implying that fainter objects are generally galaxies. This argument has been used to reclassify the very faint ($r \geqslant 21$) objects from the CCD observations by Peacock *et al.* (1981) as G?. We have 24 cases of G? identifications, and of course the foregoing argument is statistical; a few of them may be QSOs, and this must be investigated.

The optical magnitudes are inhomogeneous, having been obtained in different broad-band colours by many observers using a variety of techniques. We have attempted to quote V magnitudes in all cases by adopting relations $V–R=B–R=1$ for G/G? and $V–R=B–V=0$ for Q/Q?. In general, no distinction has been made between various roughly equivalent systems (e.g. B, m_J, m_{pg}), but for CCD r magnitudes there is a significant zero-point offset between the r and R scales; we have assumed $r–R=0.8$. For galaxies with $z \lesssim 0.01$, we used a redshift corrected for the motion of the local group as carried out by Sandage & Tammann (1981). More recent redshifts not included in the Véron-Cetty & Véron compilation were taken from Danziger & Goss 1983 (0025–23); Fricke, Kollatschny & Witzel 1983 (0451–28, 0454–46, 0834–20); Murdoch, Hunstead & White 1984 (1017–42, 2052–47); Bartel *et al.* 1984 (2021+61). Finally, to the published redshift data we added results kindly communicated to us by S. J. Lilly, H. Spinrad, B. J. Wilkes and P. Shaver.

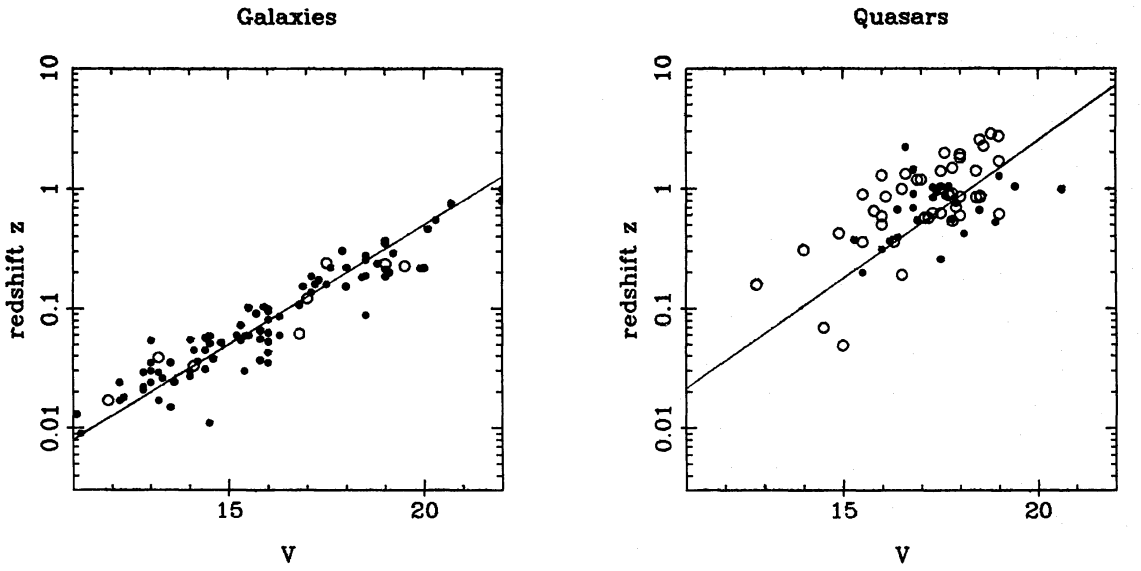

Figure 2. 'Hubble' plots (redshift versus magnitude) for galaxies and QSOs of the present catalogue. Open circles denote flat-spectrum sources; filled circles steep-spectrum.

3 Analysis

3.1 HUBBLE DIAGRAMS

Fig. 2a and b show Hubble diagrams for galaxies and QSOs of the sample, using the redshifts and V magnitudes from Table 1. The principal reason for their compilation is to provide relations from which to estimate redshifts for sample members for which such data do not exist. Despite the low accuracy of much of the photometry, there are clear correlations for both classes of optical object. The lines shown on Fig. 2 represent the mean V–z relations:

$\log_{10}(z)=0.20\,V-4.3$, (G),

$\log_{10}(z)=0.23\,V-4.2$. (Q).

If the sources with missing redshifts are a representative subsample, then it is legitimate to use the above relations to estimate redshifts. Fig. 2 suggests that this process will be accurate to within a factor 2 for galaxies and a factor 3 for QSOs in essentially all cases. Problems would arise if the objects lacking redshifts were much fainter than the range of V for which our V–z relation is defined, but this is not generally the case. Uncertainties of the above order should not affect the luminosity-function analysis given the relatively small number of sources involved. The main point is that the empirical use of magnitude as a redshift indicator should be unbiased. The correlation for the QSOs is weak, but real (see below), and our procedure is then some improvement on simply assigning $z=1$ to all QSO candidates (PWI; Wall, Pearson & Longair 1981). To complete our list of best-guessed redshifts, we must consider the empty fields and, in line with the preceding discussion of G? objects, we assume these to be galaxies below the plate limit. Experience with deep imaging (e.g. Peacock *et al.* 1981) suggests that most will be only ~1 mag below the relevant optical limit, and we have thus assumed redshifts according to the depth of the optical observations: $z=1.0$ (Palomar Survey); $z=1.6$ (UK Schmidt Survey); $z=2.0$ (CCD). Although in some cases our estimates will be grossly incorrect, in general they are accurate enough for the analyses in following sections of this paper. But it is clearly important for more redshifts to be measured.

The Hubble relation for radio galaxies is well known (although unexplained), but the existence of a similar relation for our QSOs is surprising. The QSO Hubble plot is usually thought of as a

scatter diagram. While this is certainly the case for optically selected QSOs (e.g. Schmidt & Green 1983), evidence has existed for some time that there is a correlation for radio-selected samples; Wills & Lynds (1978), for instance, found significant Hubble relations in several independent samples. The situation is, however, entirely different from that for the radio galaxies, for which radio emission somehow selects out the *top* of the optical luminosity function. The most luminous optically selected QSOs are $\geqslant 2$ mag more luminous than the most optically luminous QSO in our sample. In fact, it is the *lower* bound in luminosity which is in common to the radio and optical samples, corresponding perhaps to the point at which the objects are no longer classified as stellar but appear as N-galaxies or Seyferts. Given this, the *upper* bound to our QSO Hubble plot will be produced by any steep optical luminosity function and is thus simply a selection effect. We have considered a single V–z relation for all QSOs, although Wills & Lynds (1978) suggested that flat-spectrum QSOs were on average of higher optical luminosity. Given the scatter introduced by poor photometry, it is not surprising that there is little evidence for such an effect in Fig. 2b.

If the absolute magnitude for radio QSOs is approximately constant, there are some interesting implications. The fact that our magnitude distribution peaks at $V \simeq 18$ is then a reflection of the fact that this sample contains very few objects with $z \geqslant 2$. A naive extrapolation yields $z=4$ at $V \simeq 21$ and suggests that the upper bound would only exceed $z=4$ for $V \simeq 19$. Thus, the failure to detect high-z radio QSOs in other searches may be due to a failure to examine enough faint candidates. In this context, It is interesting to note that QSO candidates in deeper surveys (which yield more high-z objects; see Section 3.5) are indeed generally fainter, with magnitude distributions peaking at $V \simeq 20$ (e.g. Allington-Smith *et al.* 1982).

3.2 REDSHIFT DISTRIBUTIONS

Fig. 3 shows redshift distributions for the steep- and flat-spectrum sources of the present catalogue, together with these distributions for the sources in the range 1.5–2 Jy from the Northern Hemisphere sample of PWI (updated as described in Section 2). These diagrams are equivalent to luminosity distributions because the great majority of the sources have flux

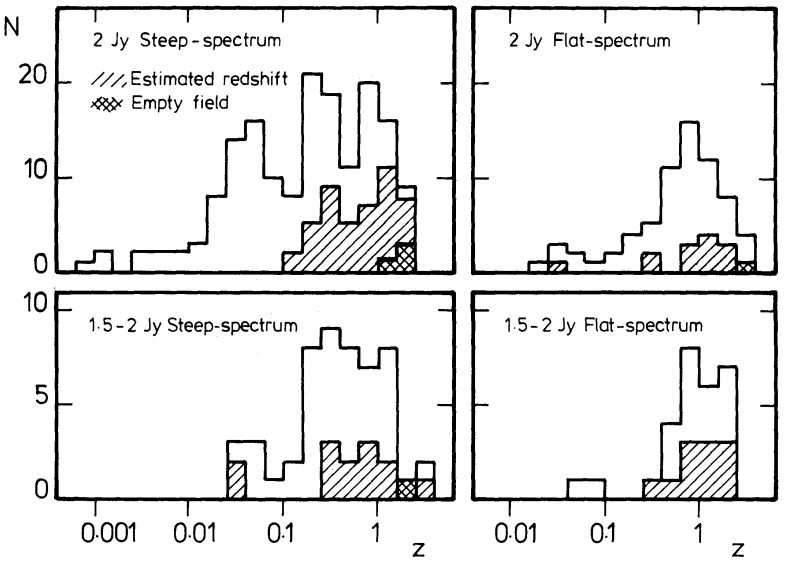

Figure 3. Redshift distributions for steep- and flat-spectrum sources for the present (2-Jy) sample and for the objects between 1.5 and 2 Jy in the northern hemisphere sample of PWI. These are equivalent to luminosity distributions because most sources have flux densities within a factor of 2 of catalogue limits.

densities within a factor of 2 of the catalogue limit. The flat-spectrum source distributions at 1.5 and 2.0 Jy are very similar. But the steep-spectrum distributions differ markedly, with the 2-Jy sample showing an increased proportion of low-luminosity objects significant at the 1 per cent level (Kolmogorov–Smirnov test). In fact the difference may be seen in the median redshifts, which are 0.17 for the 2.0-Jy sample and 0.40 for the fainter sample; this is not due to redshift estimates. The change over such a small range in flux density has significant implications for the different luminosity functions for the flat- and steep-spectrum source populations, as discussed in Section 3.5.

3.3 THE P–α (z–α) RELATION

The (z–α) diagram (equivalent to P–α for our sample, Section 3.2) for the steep-spectrum sources is shown in Fig. 4. There is a correlation which is much weaker than that noted by Laing & Peacock (1980) for the PWI 1.5-Jy sample: the Spearman rank correlation coefficient of 0.11 fails to be significant at the 10 per cent level. The difference is undoubtedly due to the exclusion by Laing & Peacock of steep-spectrum compact sources which form substantial portions of samples selected at high frequencies (Kapahi 1981; PWII). These sources show curvature of their radio spectra with broad maxima in the 0.5- to 2.0-GHz range, possibly due to synchrotron self-absorption in steep-spectrum cores or double hotspots (see van Breugel 1984 for an alternative explanation). The curvature flattens the mean spectrum of such sources at centimetre wavelengths; the resultant low $\alpha_{2.7}^{5}$ for such high-power sources places them in the lower right corner of Fig. 4, weakening the correlation which is so well established for classical double sources of the Fanaroff–Riley (1974) type II.

There has been controversy over the interpretation of the P–α relation. Laing & Peacock (1980) argued that the relation was fundamentally with luminosity, not redshift, because the correlation was well-defined at low z; there would be no time for an epoch-dependent effect to operate here. However, Macklin (1982) applied an elegant statistical method which allowed for the strong P–z correlation in flux-density-limited samples, and concluded that the reverse was true. Macklin's method quantifies the intuitive approach: the basic relation is taken to be the one with the higher correlation coefficient, which was z–α for his data. The difficulty with this analysis is that it cannot incorporate observational error. In this instance, errors in the flux densities will

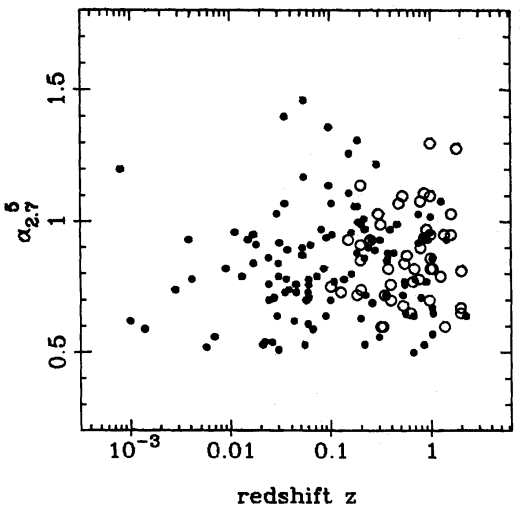

Figure 4. the spectral-index versus redshift diagram for steep-spectrum sources in the present sample, equivalent to the (P–α) presentation; see caption to Fig. 3. Open circles denote an estimated redshift.

dilute the strength of any P–α relation relative to z–α. Macklin (private communication) confirms that this has occurred, and the effect of flux density errors is sufficiently strong that a choice between P–α and z–α cannot be made. The question will only be settled by examining much deeper surveys, so that we can compare objects of the same luminosity at greatly differing redshifts.

3.4 SOURCE COUNTS

Wall (1977) used the first nine zones of the Parkes 2.7-GHz survey to compile counts for all sources at 2.7 GHz, and for flat- and steep-spectrum sources independently. We have revised these counts by adding results from the present catalogue, PWI (revised as in Section 2), from the remaining five zones of the Parkes survey and from recent observations of the selected-area surveys (Downes *et al.*, in preparation). The results are given in Table 2 and Fig. 5; very good definitions of surface-density laws are apparent for the individual populations down to 100 mJy. The error bars above 1.5 Jy are as small as they will ever be, now that there exists complete sky coverage to that level. For low flux densities, spectral data are now available for essentially all sources, and the spectrally separated counts can be constructed directly, in contrast with Wall *et al.* (1981) who used some limited spectral data to estimate the *proportion* of the two types in the total count.

The total counts (Fig. 5) show the familiar features of normalized differential counts at all frequencies – an initial rise at a rate exceeding the (Euclidean) $-3/2$ power law, a plateau, and a decline which is confirmed to continue to lower flux densities by $P(D)$ analysis at 2.7 GHz (Wall & Cooke 1975 and unpublished data), and by deep surveys at both 1.4 and 5.0 GHz (Wall 1983). The plateau is broader than that apparent in low-frequency counts (e.g. 408 MHz), and the reason for this is the presence of the two populations at cm-wavelengths, which provide two different counts of similar form (Fig. 5) but with maxima displaced in flux density, the displacement increasing with frequency (Wall & Benn 1982).

One of the most interesting comparisons between the counts is of their slopes. Above ~1 Jy, Fig. 5 shows that both spectral populations have counts significantly steeper than Euclidean, but

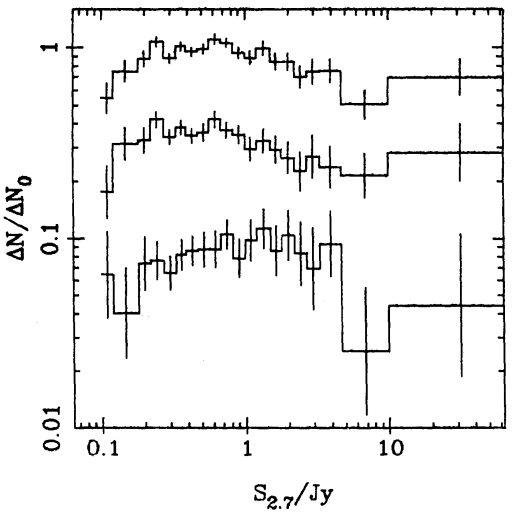

Figure 5. Source counts in relative differential form (top) for all sources at 2.7 GHz, (centre) for steep-spectrum sources, and (bottom) for flat-spectrum sources, divided at a spectral index $\alpha_{2.7}^{5}$ of 0.5. The normalization is to 100 $S^{-1.5}$, and for clarity, the steep-spectrum and flat-spectrum counts have been displaced downwards by factors of 2 and 3 respectively relative to the numbers in Table 2.

Table 2. 2.7-GHz source counts.

$S_{2.7}$/Jy	Area/sr	Steep-Spectrum ΔN	Steep-Spectrum $\Delta N/\Delta N_o$	Flat-Spectrum ΔN	Flat-Spectrum $\Delta N/\Delta N_o$	Total ΔN	Total $\Delta N/\Delta N_o$
∞							
	9.81	17	0.549	4	0.129	21	0.678
10.00							
	9.81	8	0.329	3	0.123	11	0.453
6.80							
	9.81	21	0.512	2	0.049	23	0.561
4.70							
	9.81	32	0.475	18	0.267	50	0.742
3.30							
	9.81	31	0.539	12	0.209	43	0.748
2.70							
	9.81	36	0.453	20	0.252	56	0.704
2.20							
	9.81	56	0.530	33	0.313	89	0.843
1.80							
	9.81	75	0.587	33	0.258	108	0.845
1.50							
	6.95	98	0.652	51	0.339	149	0.991
1.20							
	6.95	98	0.589	49	0.295	147	0.884
1.00							
	6.95	169	0.701	57	0.237	226	0.938
0.82							
	6.95	225	0.741	96	0.316	321	1.058
0.68							
	3.77	192	0.845	60	0.264	252	1.109
0.56							
	3.77	195	0.721	71	0.263	266	0.984
0.47							
	3.77	262	0.693	98	0.259	360	0.953
0.39							
	3.05	274	0.768	88	0.247	362	1.015
0.33							
	1.97	249	0.682	72	0.197	321	0.879
0.27							
	0.966	209	0.844	57	0.230	266	1.074
0.22							
	0.372	83	0.656	28	0.221	111	0.877
0.18							
	0.0753	52	0.630	10	0.121	62	0.751
0.12							
	0.0753	20	0.351	11	0.193	31	0.544
0.10							

$$\Delta N_o = 100\, S_{2.7}^{-1.5}\ \mathrm{sr}^{-1}$$

there is some suggestion that this may flatten at the highest flux densities. To perform the comparison quantitatively, we use the well-known method of maximum likelihood (ML) to fit a form $dN \propto S^{-\beta}$ to the counts. Clearly we wish to fit over a restricted range of flux densities, so that the variation of β with S may be examined. If the range of S is too small, only a few sources are taken at any one time and the error bars in β will be large. Thus, we must specify an averaging scale which is as large as possible consistent with not smearing-out features of interest in the counts; we have taken this to be a factor of 10 in flux density. With differential counts of the form $AS^{-\beta}$ normalized over the range (S_1, S_2), the likelihood L is given by

$$-\ln L = (\beta-1)\sum_i \ln (S_i/S_1) + N \ln\left[\frac{1-R^{-(\beta+1)}}{(\beta-1)}\right] \qquad (1)$$

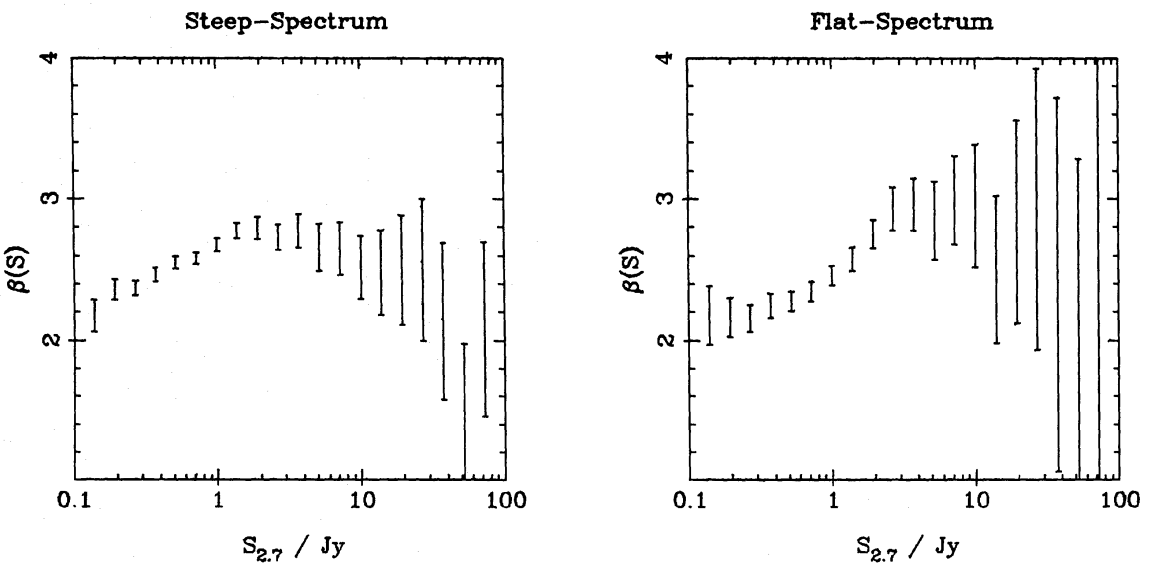

Figure 6. Maximum-likelihood slopes β for the source counts, $dN \propto S^{-\beta}$, steep- and flat-spectrum sources. The averaging length is a factor of 10 in S.

where $R=S_2/S_1$. The best-fitting value of β is found by solving $\partial L/\partial\beta=0$ and error bars on β are given by $(\partial^2 \ln L/\partial\beta^2)^{-1/2}$. Fig. 6 shows the results for the variation of $\beta(S)$; points are plotted more frequently than a factor of 10 in S and are thus not all independent. Although both counts are equally steep at moderately high flux densities ($\beta \simeq 2.8$ at $S \simeq 3$ Jy), the steep-spectrum population shows a return to values consistent with Euclidean at the highest flux densities. The error bars on $\beta(S)$ for the flat-spectrum population are sufficiently large that we cannot say whether it also becomes asymptotically Euclidean at this level. The interpretation of these results falls into the domain of the luminosity function, which we now consider.

3.5 LUMINOSITY FUNCTIONS

The fundamental data from which we may deduce the luminosity function are the values of S and z for each source. Fig. 7 shows the distributions of these points over the S–z planes for steep- and

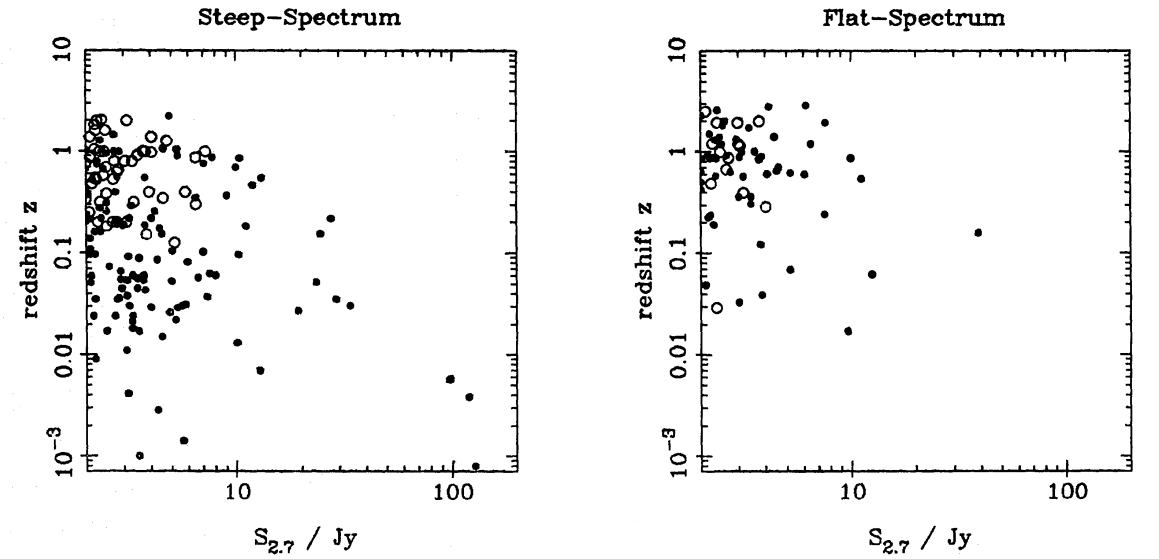

Figure 7. The S–z planes for steep- and flat-spectrum sources. Open circles denote estimated redshifts.

flat-spectrum sources separately. Both of these diagrams demonstrate a correlation in the sense that the very brightest sources are also those of lower redshift, the effect being most marked in the case of the steep-spectrum population. This is a statement that the source counts for objects in a fixed redshift range, $dN(S, z)$, are steeper at high redshift. Since, at constant z, flux density and luminosity are in a fixed ratio, this corresponds to saying that the luminosity function is steeper at high z. We may quantify this by using the ML technique of Section 3.4 to deduce the slopes involved. We now place no restriction on S but consider sources in a range of z to find $\beta(z)$; we take again an averaging scale of a factor 10 in z. Fig. 8a shows the result: at low redshifts, both spectral types have luminosity functions $\varrho(P) \sim P^{-2}$, but in both cases this steepens to $\sim P^{-3}$ at high redshift (i.e. luminosity). (The slopes β derived here are greater by one than slopes derived when luminosity functions are derived per unit log P.) This in itself does not yet establish curvature of the RLF because of the different redshifts involved, as discussed below.

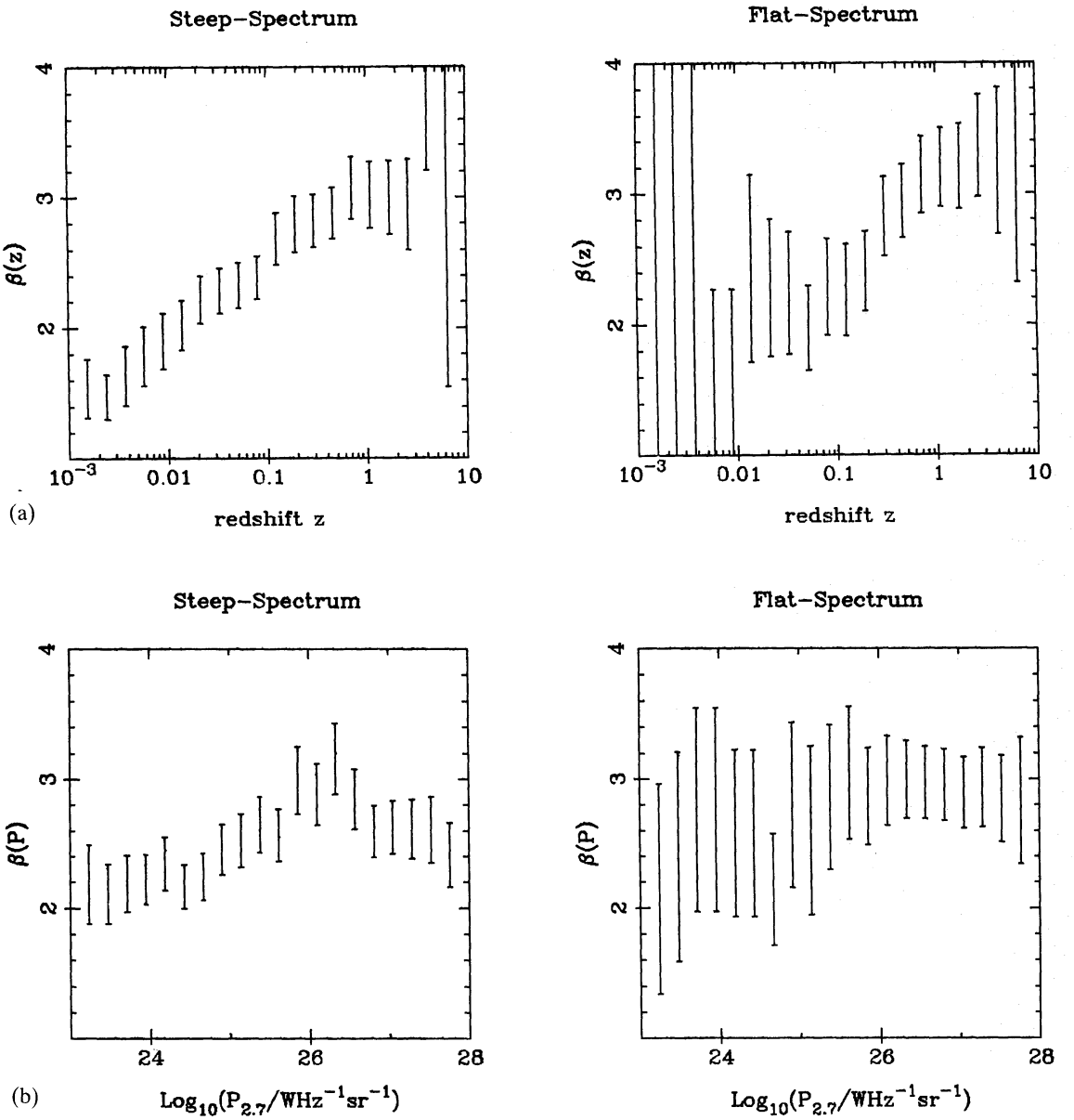

Figure 8. (a) Maximum-likelihood slopes for the redshift-dependent source counts $\beta(z)$ where $dN(S, z) \propto S^{-\beta(z)}$, steep- and flat-spectrum sources. The averaging length is a factor of 10 in z. (b) As for (a) but $\beta(P)$, with averaging over $\Delta \log_{10}(P) = 1.5$.

Moroever, the behaviour says nothing about the *evolution* of the luminosity function. For that, we must instead consider sources in a fixed range of luminosity. We can perform the analogous exercise to the above, but now considering the *S–P* plane and using ML to find $\beta(P)$; and the results (assuming H_0=50 km s^{-1} Mpc^{-1}, q_0=0.5) are shown in Fig. 8b. The differential behaviour of Fig. 8a is largely absent; $\beta(P)$ shows an increase of ~0.5 to a maximum of $\beta(P)\simeq 2.8$ at high P for steep-spectrum sources. No such behaviour is apparent for the flat-spectrum population, but because a more restricted range of luminosity is sampled, it would be hard to detect. It is important to note that $\beta(z)$ and $\beta(P)$ are remarkably similar, despite their complete independence. This difficulty of distinguishing evolutionary effects from ones intrinsic to the shape of the luminosity function may help to explain why the interpretation of the number counts alone was long a source of controversy. Certainly, these trends allow us to understand the Euclidean slope at high flux densities (Fig. 6a); at this level the steep-spectrum population is becoming dominated by nearby low-luminosity sources such as For A, Pic A, Cen A, etc. It is sad that we will never have the statistics to determine whether the flat-spectrum population shows such behaviour at low redshifts.

So far, we have regarded Fig. 8b as empirical and have not interpreted it in terms of changing space densities. The high values of $\beta(P)$ clearly indicate that ϱ increases to higher z. How fast? A quantitative answer may be obtained by assuming that the time dependence is of the form $\varrho \propto \exp(m\tau)$, where τ is the look-back time in units of the age of the Universe. $\beta(P)$ is closely related to m, so we may derive a luminosity-dependent measure of the strength of the evolution $m(P)$. *This is not a model-dependent answer*: as most sources lie close to the sample limit, m can be thought of as giving simply a local value of $\partial \ln \varrho/\partial\tau$. We may derive $m(P)$ by using the V'_e/V'_a technique of Avni & Bahcall (1980). This defines a variable related to the classical V/V_{max}, but incorporating an assumed form of variation in ϱ with z. Thus consistent forms for $\varrho(z)$ are taken to be those for which $\langle V'_e/V'_a\rangle$ for a sample of N sources is equal to 0.5 to within the statistical error $(12N)^{-1/2}$. The analysis proceeds as for $\beta(P)$: objects in a range $\Delta \log_{10} P$=1.5 are considered and the allowed range of $m(P)$ for that bin is deduced. The resulting limits on $m(P)$ are plotted in Fig. 9. Only results for high luminosities are shown, since the data at low redshift are very insensitive to $m(P)$; for limiting redshifts $z \ll 1$, $\beta(P) \to 2.5$, whatever m may be ($\Delta\beta \simeq 0.75mz$ for q_0=0.5 and

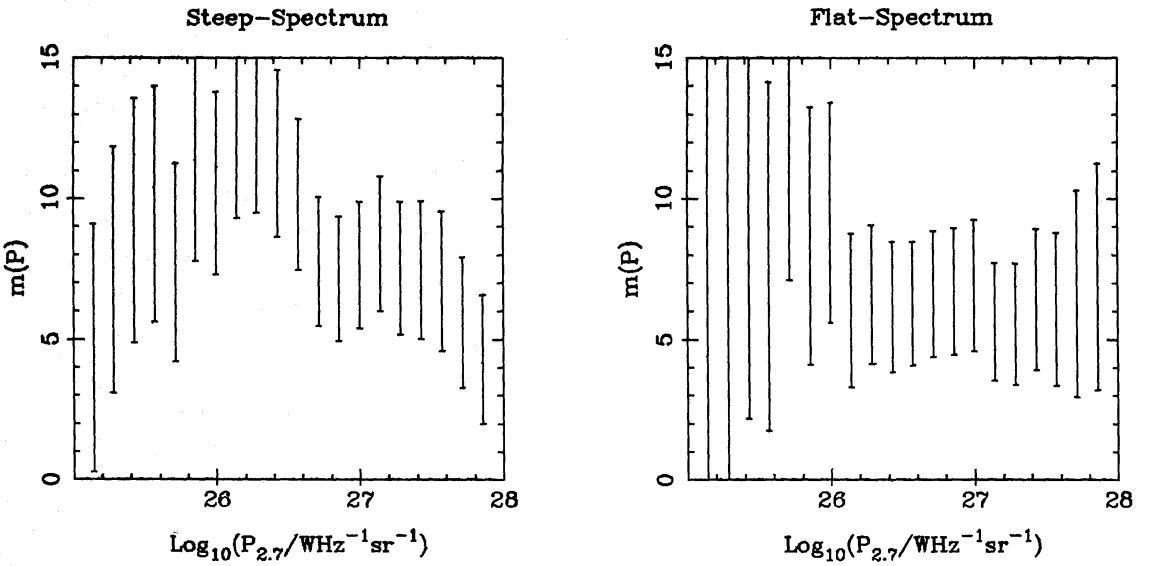

Figure 9. Values of the radio luminosity function slope $m=\partial \ln \varrho/\partial\tau$ at our sample limit as a function of P, steep- and flat-spectrum sources. The averaging length is $\Delta \log_{10}(P)$=1.5. This is a *local* look at the behaviour, and does not assume $\varrho \propto \exp(m\tau)$ for all redshifts. Only q_0=0.5 is shown; the results for q_0=0 are similar apart from a factor 1.5 in m (for q_0=0.5, $\tau=1-(1+z)^{-1.5}\simeq 1.5\ z$; for q_0=0, $\tau=1-(1+z)^{-1}\simeq z$).

$\simeq 0.5mz$ for $q_0=0$). In fact, $\beta(P)\leqslant 2.5$ for steep-spectrum sources with $P\leqslant 10^{24}$ W Hz^{-1} sr^{-1} and the best-fitting values of m in this region are large and negative. The errors, though, are large and $m=0$ is not excluded; nevertheless it is possible that the slightly sub-Euclidean values of $\beta(P)$ here are due to a remaining incompleteness of low-luminosity diffuse sources close to our sample limit. At higher luminosities, the situation is clear, with values of $m(P)\simeq 7$–10 indicating strong evolution. Above $P=10^{25}$ W Hz^{-1} sr^{-1}, there is no evidence for a variation of $m(P)$ with P; the mean values of $m(P)$ in this range are 8.0 ± 2.0 and 6.5 ± 2.0 for steep- and flat-spectrum populations respectively. The evolution appears stronger (i.e. higher m) for the steep-spectrum sources, but the difference is not significant and a global value of $m=7.5$ for all powerful sources would be acceptable. For sources of lower luminosity, we cannot set useful limits on m; even raising the upper luminosity limit to 10^{26} W Hz^{-1} sr^{-1} yields $m=2.1\pm 4.2$ for the 93 steep-spectrum sources below this limit, as compared to 8.6 ± 2.3 for those above it. This is suggestive of differential evolution, but does not rule out $m=8$ at low luminosities, for the reasons discussed above. To obtain a direct limit on m for low-luminosity sources, we need to see objects with $P\sim 10^{25}$ W Hz^{-1} sr^{-1} out to $z\sim 1$, only possible in samples ~ 100 times fainter than the present one. For now, we cannot improve on the indirect arguments which imply slow changes in the RLF at lower luminosities from the rapid convergence of the source counts.

Finally, differential evolution has an interesting consequence for the luminosity function, which we showed above to be curved in the sense that it is steeper for sources of high luminosity *at high redshift* than for nearby sources of low luminosity. Since differential evolution increases ϱ at high z for the powerful sources only, this will introduce curvature in the opposite sense to that observed. Thus, we may infer that the *local* luminosity function is even more strongly curved: the present slope for high-P sources may correspond to $\beta\simeq 5$ (*cf.* the model local RLFs of Peacock & Gull 1981). This extreme curvature is far more suggestive of, for example, an exponential cut-off than of a transition between different power laws. This would then be analogous to the galaxy optical luminosity function which has a sharp upper limit (e.g. Felten 1977).

4 Conclusions

The all-sky catalogue contains the 233 brightest extragalactic radio sources at 2.7 GHz; it is complete to 2.0 Jy over 9.81 sr of sky. There are 227 optical identifications, and 171 measured redshifts. The completeness of the data led to development of a maximum-likelihood technique to explore the implications for the source populations. This has enabled several features of the luminosity functions and their epoch dependence to be demonstrated with improved accuracy: (i) the significant flattening of the counts for steep-spectrum sources at the highest flux densities, (ii) the existence of strong curvature in the luminosity functions of both steep- and flat-spectrum sources at high redshifts, and (iii) the strong cosmological evolution for powerful flat-spectrum sources. Taken in conjunction with the low evolution found for flat-spectrum sources of moderate luminosity (Wall *et al.* (1981), this latter result confirms differential evolution for flat-spectrum sources as proposed by Peacock *et al.* (1981) and Peacock & Gull (1981).

It is interesting to note that these conclusions are possible from the present sample of 233 sources alone. Although further analyses involving deeper samples will provide a still more detailed picture of the space distributions and evolutionary changes of the radio-source population, this work has taken our knowledge of the spatial distribution of *nearby* powerful sources up to a fundamental statistical limit.

Acknowledgments

We thank Drs Véron and Véron-Cetty for supplying a preprint of their invaluable compilation of radio-source identifications and Robert Laing for very helpful discussions. The Parkes 2.7-GHz

survey began in 1967 at John Bolton's instigation, and an all-sky catalogue is in a sense a culmination of this work; we pay tribute to his foresight and inspiration.

References

Adgie, R. L., Crowther, J. H. & Gent, H., 1972. *Mon. Not. R. astr. Soc.,* **159,** 233.

Allington-Smith, J. R., Perryman, M. A. C., Longair, M. S., Gunn, J. E. & Westphal, J. A., 1982. *Mon. Not. R. astr. Soc.,* **201,** 331.

Avni, Y. & Bahcall, J. N., 1980. *Astrophys. J.,* **235,** 694.

Bartel, N., Shapiro, I. I., Huchra, J. P. & Kühr, H., 1984. *Astrophys. J.,* **279,** 112.

Birkinshaw, M., Laing, R. A. & Peacock, J. A., 1981. *Mon. Not. R. astr. Soc.,* **197,** 253.

Bolton, J. G., Wright, A. E. & Savage, A., 1979. *Aust. J. Phys. Astrophys. Suppl.,* **46.**

Bridle, A. H., Davis, M. M., Fomalont, E. B. & Lequeux, J., 1972. *Astr. J.,* **77,** 405.

Burbidge, G. & Crowne, A. H., 1979. *Astrophys. J. Suppl.,* **40,** 583.

Burch, S. F., 1979. *Mon. Not. R. astr. Soc.,* **186,** 519.

Cameron, M. J., 1971. *Mon. Not. R. astr. Soc.,* **152,** 439.

Christiansen, W. N., Frater, R. H., Watkinson, A., O'Sullivan, J. D., Lockhart, I. A. & Goss, W. M., 1977. *Mon. Not. R. astr. Soc.,* **181,** 183.

Danziger, I. J. & Goss, W. M., 1983. *Mon. Not. R. astr. Soc.,* **202,** 703.

Ekers, R. D., Goss, W. M., Kotanyi, C. G. & Skellern, D. J., 1978. *Astr. Astrophys.,* **69,** L21.

Elsmore, B. & Ryle, M., 1976. *Mon. Not. R. astr. Soc.,* **174,** 411.

Fanaroff, B. L. & Riley, J. M., 1974. *Mon. Not. R. astr. Soc.,* **167,** 31P.

Felten, J. E., 1977. *Astr. J.,* **82,** 861.

Fomalont, E. B. & Moffet, A. T., 1971. *Astr. J.,* **76,** 5.

Fricke, K. J., Kollatschny, W. & Witzel, A., 1983. *Astr. Astrophys.,* **117,** 60.

Hargrave, P. J., 1974. *Mon. Not. R. astr. Soc.,* **168,** 491.

Hargrave, P. J. & McEllin, M., 1975. *Mon. Not. R. astr. Soc.,* **173,** 37.

Hewitt, A. & Burbidge, G., 1980. *Astrophys. J. Suppl,* **43,** 57.

Hunstead, R. W., 1972. *Mon. Not. R. astr. Soc.,* **157,** 367.

Jenkins, C. J., Pooley, G. G. & Riley, J. M., 1977. *Mem. R. astr. Soc.,* **84,** 61.

Kapahi, V. K., 1981. *Astr. Astrophys. Suppl.,* **43,** 381.

Kellermann, K. I., Pauliny-Toth, I. I. K. & Tyler, W. C., 1968. *Astr. J.,* **73,** 298.

Kühr, H., Witzel, A., Pauliny-Toth, I. I. K. & Nauber, U., 1981. *Astr. Astrophys. Suppl.,* **45,** 367.

Laing, R. A., 1981. *Mon. Not. R. astr. Soc.,* **195,** 261.

Laing, R. A. & Peacock, J. A., 1980. *Mon. Not. R. astr. Soc.,* **190,** 903.

Laing, R. A., Riley, J. M. & Longair, M. S., 1983. *Mon. Not. R. astr. Soc.,* **204,** 151.

Large, M. I., Mills, B. Y., Little, A. G., Crawford, D. F. & Sutton, J. M., 1981. *Mon. Not. R. astr. Soc.,* **194,** 693.

Longair, M. S., 1975. *Mon. Not. R. astr. Soc.,* **173,** 309.

Macklin, J. T., 1982. *Mon. Not. R. astr. Soc.,* **199,** 1119.

Mayer, C. J., 1979. *Mon. Not. R. astr. Soc.,* **186,** 99.

Morabito, D. D., Preston, R. A., Slade, M. A. & Jauncey, D. L., 1982. *Astr. J.,* **87,** 517.

Morabito, D. D., Preston, R. A., Slade, M. A., Jauncey, D. L. & Nicolson, G. D., 1983. *Astr. J.,* **88,** 1138.

Murdoch, H. S., Hunstead, R. W. & White, G. L., 1984. *Proc. ASA,* **5,** 341.

Northover, K. J. E., 1973. *Mon. Not. R. astr. Soc.,* **165,** 369.

Northover, K. J. E., 1976. *Mon. Not. R. astr. Soc.,* **177,** 307.

Pauliny-Toth, I. I. K., Wade, C. M. & Heeschen, D. S., 1966. *Astrophys. J. Suppl.,* **13,** 65.

Peacock, J. A. & Gull, S. F., 1981. *Mon. Not. R. astr. Soc.,* **196,** 611.

Peacock, J. A. & Wall, J. V., 1981. *Mon. Not. R. astr. Soc.,* **194,** 331 (PWI).

Peacock, J. A. & Wall, J. V., 1982. *Mon. Not. R. astr. Soc.,* **198,** 843 (PWII).

Peacock, J. A., Perryman, M. A. C., Longair, M. S., Gunn, J. E. & Westphal, J. A., 1981. *Mon. Not. R. astr. Soc.,* **194,** 601.

Perley, R. A., 1982. *Astr. J.,* **87,** 859.

Pooley, G. G. & Henbest, S. N., 1974. *Mon. Not. R. astr. Soc.,* **169,** 477.

Prestage, R. M. & Peacock, J. A., 1983. *Mon. Not. R. astr. Soc.,* **204,** 355.

Riley, J. M. & Branson, N. J. B. A., 1973. *Mon. Not. R. astr. Soc.,* **164,** 271.

Riley, J. M. & Pooley, G. G., 1975. *Mem. R. astr. Soc.,* **80,** 105.

Robertson, J. G., 1973. *Astr. J. Phys.,* **26,** 403.

Sandage, A. R. & Tammann, G. A., 1981. In: *A Revised Shapley–Ames Catalog of Bright Galaxies,* Carnegie Institution, Washington.
Schilizzi, R. T. & McAdam, W. B., 1975. *Mem. R. astr. Soc.,* **79,** 1.
Schmidt, M. & Green, R. F., 1983. *Astrophys. J.,* **269,** 352.
Smith, H. E. & Spinrad, H., 1980. *Publs astr. Soc. Pacif.,* **92,** 553.
Spinrad, H., Stauffer, J. & Butcher, H., 1981. *Astrophys. J.,* **244,** 382.
Turland, B. D., 1975. *Mon. Not. R. astr. Soc.,* **170,** 281.
Ulvestad, J., Johnson, K., Perley, R. & Fomalont, E., 1981. *Astr. J.,* **86,** 1010.
van Breugel, W., 1984. In: *VLBI and Compact Radio Sources, IAU Symp. No. 110,* p. 59, eds Fanti, R., Kellermann, K. & Setti, G., Reidel, Dordrecht, Holland.
Véron-Cetty, M. P. & Véron, P., 1983. *Astr. Astrophys. Suppl.,* **53,** 219.
Waggett, P. C., Warner, P. J. & Baldwin, J. E., 1977. *Mon. Not. R. astr. Soc.,* **181,** 465.
Wall, J. V., 1977. In: *Radio Astronomy and Cosmology, IAU Symp. No. 74,* p. 55, ed. Jauncey, D. L., Reidel, Dordrecht, Holland.
Wall, J. V., 1983. In: *The Origin and Evolution of Galaxies,* p. 295, eds Jones, B. J. T. & Jones, J. E., Reidel, Dordrecht, Holland.
Wall, J. V. & Benn, C. R., 1982. In: *Extragalactic Radio Sources, IAU Symp. No. 97,* p. 441, eds Heeschen, D. S. & Wade, C. M., Reidel, Dordrecht, Holland.
Wall, J. V. & Cooke, D. J., 1975. *Mon. Not. R. astr. Soc.,* **171,** 9.
Wall, J. V., Pearson, T. J. & Longair, M. S., 1981. *Mon. Not. R. astr. Soc.,* **196,** 597.
Willis, A. G., Strom, R. G. & Wilson, A. S., 1974. *Nature,* **250,** 625.
Wills, D. & Lynds, R., 1978. *Astrophys. J. Suppl.,* **36,** 317.